

# POSITION CONTROL OF ROBOTIC MANIPULATOR JOINTS WITH TWO DEGREES OF FREEDOM USING SDRE CONTROL

FREDERIC CONRAD JANZEN<sup>1</sup>, DANIEL KOSLOPP<sup>1</sup>, TALITA TOBIAS CARNEIRO<sup>1</sup>, CLAUDINOR BITENCOURT NASCIMENTO<sup>1</sup>, FELIPE BARRETO CAMPELO CRUZ<sup>1</sup>, ANGELO MARCELO TUSSET<sup>1</sup>, JOSÉ MANOEL BALTHAZAR<sup>2</sup>

1. Departamento de Eletrônica, UTFPR

Correspondence Address

E-mails: [fcjanzen@utfpr.edu.br](mailto:fcjanzen@utfpr.edu.br), [koslopp@gmail.com](mailto:koslopp@gmail.com), [talitatobias@outlook.com](mailto:talitatobias@outlook.com), [claudinor@utfpr.edu.br](mailto:claudinor@utfpr.edu.br), [fbcruz@utfpr.edu.br](mailto:fbcruz@utfpr.edu.br), [tusset@utfpr.edu.br](mailto:tusset@utfpr.edu.br)

2. Departamento de Estatística, Matemática Aplicada e Computacional, UNESP-RC

Avenida 24A. 1515. Bela Vista, 13506-700 - Rio Claro, SP.

E-mail: [jmbaltha@rc.unesp.br](mailto:jmbaltha@rc.unesp.br)

**Abstract**— This paper presents a control design for robotic manipulators with two links. The dynamic model of the manipulator is obtained in a closed form through the Lagrange equations. The control strategy involves the application of two control signals, a nonlinear feedforward control to maintain the controlled system in a desired point, and a state feedback control, obtained by the State Dependent Riccati Equation (SDRE), to bring the system trajectory into at a desired point. The control is realized through the control of motor voltage. A state-dependent equation is solved at each new point obtained for the variables from the problem, along the trajectory to obtain a nonlinear feedback controller. Numerical simulations demonstrate the effectiveness of the control strategy in leading the system from any initial condition to a desired point.

**Keywords**— Optimal Control, SDRE Control, Nonlinear Control, Robot Control, Robotic Manipulator

## 1 Introduction

The main objective of the control of a robot is to manipulate objects precisely, where inputs receive the position and speed that are provided by sensors localized at specific points of the manipulator, so then calculate and apply the necessary force, to perform the desired movement.

Robotic systems are modeled as linear with respect to parameters as mass, inertia, and damping factors, but this assumption is not valid for the state, requiring nonlinear control design (Molter et al., 2010). And of according to (Hashemipour et al., 2013) robotic trajectory control is a very complicated problem, due to the coupled and nonlinear system dynamics.

The presence of nonlinearities and the consequent nonlinear behavior exhibited by robot parts is a problem that gives rise to serious difficulties in the kinematics and especially the dynamic modeling, analysis and control of robotic joints (Cassiano and Balthazar, 2007).

The SDRE control is among the techniques that emerged to deal with highly non-linear and complex systems, such as the control of robotic dynamics (Fenili and Balthazar, 2009; Korayem et al, 2011). The procedure to drive the tip position to a desired point via SDRE technique can consider successive optimal solutions for static equations and feedback control stabilized system.

In Huifeng et al. (2011) swinging-up and stabilization problem of a single inverted pendulum on a cart is considered via SDRE controller and it is ex-

plained that the design flexibility is the greatest advantage of using SDRE.

In this paper we propose the positioning control technique for a robot, with two links, where the motor torque controls the joint angle tracking. Simulation was created to assess the control model feasibility and efficiency.

## 2 Mathematical model

### 2.1 Manipulator model

The mathematical model of the robotic manipulator can be represented by Fig. 1:

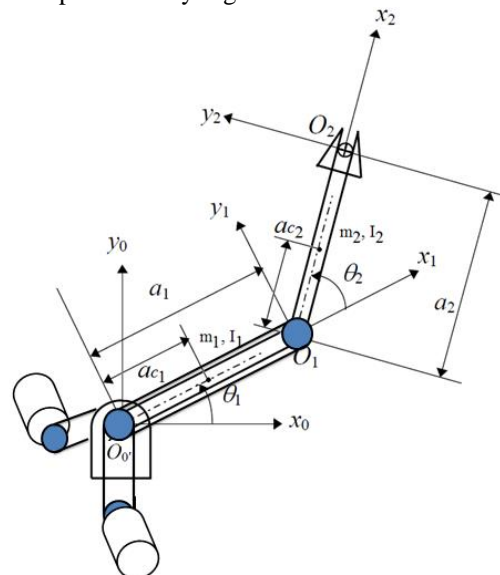


Figure 1. Planar robot with two degrees of freedom (Korayem et al, 2011)

The mathematical model of the robotic manipulator can be obtained through the Euler-Lagrangian method. The Lagrangian is defined by the equation:

$$L = K - V \quad (1)$$

where K is the kinetic energy and V the potential energy.

The equations of Euler-Lagrange are expressed by:

$$\tau_j = \frac{d}{dt} \frac{\partial L}{\partial \dot{q}_j} - \frac{\partial L}{\partial q_j} \quad (2)$$

Where  $\tau_j$  is the non-conservative generalized force independent of  $q_j$ , so every freedom degree of the system will have a Lagrangian, in other words, a system of n differential equations for n freedom degrees.

So the dynamic equations of the system can be written as:

$$\begin{aligned} d_{11}\ddot{\theta}_1 + d_{12}\ddot{\theta}_2 + c_{121}\dot{\theta}_1\dot{\theta}_2 + c_{211}\dot{\theta}_1\dot{\theta}_2 + \\ + c_{221}\dot{\theta}_2^2 + \phi_1 = \tau_1 \\ d_{21}\ddot{\theta}_1 + d_{22}\ddot{\theta}_2 + c_{112}\dot{\theta}_1^2 + \phi_2 = \tau_2 \end{aligned} \quad (3)$$

Since that  $d_-$ ,  $c_-$  and  $\phi_-$  are obtained from the following equations:

$$\begin{aligned} c_{111} = c_{122} = c_{212} = c_{222} = 0 \\ c_{121} = c_{211} = c_{221} = -m_2 a_1 a_{c2} \sin(\theta_2) \end{aligned} \quad (4)$$

$$\begin{aligned} c_{112} = m_2 a_1 a_{c2} \sin(\theta_2) \\ \phi_1 = (m_1 a_{c1} + m_2 a_1) g \cos(\theta_1) + \\ + m_2 a_{c2} g \cos(\theta_1 + \theta_2) \end{aligned} \quad (5)$$

$$\begin{aligned} \phi_2 = m_2 a_{c2} g \cos(\theta_1 + \theta_2) \\ d_{11} = m_2 (a_1^2 + a_{c2}^2 + 2a_1 a_{c2} \cos(\theta_2)) + \\ + I_1 + I_2 + m_1 a_{c1}^2 \\ d_{12} = d_{21} = m_2 (a_{c2}^2 + 2a_1 a_{c2} \cos(\theta_2)) + I_2 \\ d_{22} = m_2 a_{c2}^2 + I_2 \end{aligned} \quad (6)$$

Considering:  $x_1 = \theta_1$ ,  $x_2 = \dot{\theta}_1$ ,  $x_3 = \theta_2$  and  $x_4 = \dot{\theta}_2$ , the system (3) can also be represented in the form of state space:

$$\dot{\mathbf{x}} = \mathbf{A}(x)\mathbf{x} + \mathbf{B}(x)\mathbf{u}_r + \mathbf{G} \quad (7)$$

Where:

$$\begin{aligned} \mathbf{A} = \begin{bmatrix} 0 & 1 & 0 & 0 \\ 0 & pd_{22}(c_{211}x_4 + c_{121}x_4) & 0 & pd_{22}c_{221}x_4 \\ 0 & -pd_{12}c_{112}x_2 & 0 & 1 \\ 0 & 0 & 0 & 1 \\ 0 & pd_{11}c_{112}x_2 & 0 & -pd_{21}c_{221}x_4 \\ 0 & -pd_{21}(c_{211}x_4 + c_{121}x_4) & 0 & -pd_{21}c_{221}x_4 \end{bmatrix}, \\ \mathbf{B} = \begin{bmatrix} 0 & 0 \\ -pd_{22} & pd_{12} \\ 0 & 0 \\ pd_{21} & -pd_{11} \end{bmatrix}, \mathbf{G} = \begin{bmatrix} 0 \\ p(d_{22}\phi_1 - d_{12}\phi_2) \\ 0 \\ p(-d_{21}\phi_1 - d_{11}\phi_2) \end{bmatrix}, \\ p = \frac{1}{(d_{21}d_{12} - d_{11}d_{22})}, \mathbf{u}_r = \begin{bmatrix} \tau_1 \\ \tau_2 \end{bmatrix} \end{aligned}$$

As can be seen, the matrix  $\mathbf{A}$  depends of the states, and the control  $\mathbf{u}_r$  (feedback) that takes the system to a desired point or orbit can be obtained considering an application of a SDRE control. Due the terms of the matrix G are not dependent of the states, use only the (feedback) control is not sufficient to control this system, so is proposed the introduction of an  $\mathbf{u}_r$  (feedforward) control to maintain the system in a determined orbit (Tusset et al, 2012).

The feedforward control is obtained from:

$$\mathbf{u}_r = -\mathbf{G} \quad (8)$$

And the feedback control can be obtained from:

$$\mathbf{u}_r = -\mathbf{R}^{-1}(x)\mathbf{B}^T(x)\mathbf{P}(x)\mathbf{x} \quad (9)$$

Where  $\mathbf{P}(x)$  is obtained from the Riccati equation:

$$\begin{aligned} \mathbf{P}(x)\mathbf{A}(x) + \mathbf{A}^T(x)\mathbf{P}(x) + \mathbf{Q}(x) - \\ - \mathbf{P}(x)\mathbf{B}(x)\mathbf{R}^{-1}(x)\mathbf{B}^T(x)\mathbf{P}(x) = 0 \end{aligned} \quad (10)$$

The matrices  $\mathbf{Q}(x)$  and  $\mathbf{R}(x)$  are positive defined and are determined by the planner considering the criteria to perform the minimization of the functional:

$$J = \int_0^\infty x^T Q(x)x + u_r^T R(x)u_r dt \quad (11)$$

## 2.2 Mathematical model of the direct current motor

The motor with independent excitation is shown Figure (2).

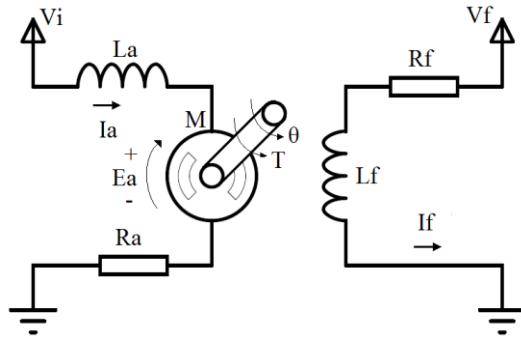


Figure 2. Motor with independent excitation (Groover et al, 1986)

Conform Groover et al (1986) a mathematical representation can be obtained from equation:

$$V_i = \left( \frac{IR}{K_e} \right) \ddot{\theta} + \left( \frac{bR}{K_e} + K_e \right) \dot{\theta} \quad (12)$$

Where  $I$  is the inertia constant of the motor,  $K_e$  the voltage constant,  $b$  the torque constant and  $R$  the resistance of the coil. To effects of simulation one motor was designed for each link.

## 3 Numerical Simulation

### 3.1 Joint positioning

The objective is determining the control signal  $u_r$  which considers the position of the joints in any initial condition and takes them to a desired position by minimizing the functional (11).

Considering the parameters of Table 1:

Table 1. Simulation Parameters.

$a_1$	$a_2$	$a_{c1}$	$a_{c2}$
0.35	0.255	0.175	0.1275
$m_1$	$m_2$	$I_1$	$I_2$
1.21799	0.6655	0.012433	0.003606

And defining the value of the matrices  $Q(x)$  and  $R(x)$  as:

$$Q = \begin{bmatrix} 100 & 0 & 0 & 0 \\ 0 & 100 & 0 & 0 \\ 0 & 0 & 100 & 0 \\ 0 & 0 & 0 & 100 \end{bmatrix} \quad R = \begin{bmatrix} 0.1 & 0 \\ 0 & 0.1 \end{bmatrix}$$

Because the matrix  $A(x)$  changes conform the states, it is necessary to verify the rank ( $r$ ) of the controllability matrix  $M$  in every interaction. If  $r < 4$  the controllable matrix  $A(x)$  obtained from last the interaction is utilized, where:

$$M = [B(x) \quad A(x)B(x) \quad \dots \quad A(x)^{n-1}B(x)] \quad (13)$$

Defining the values of the initial conditions and desired positions conform Table 2.

Table 2. Initial and desired coordinates.

$i$	$\theta_1(i)$	$\dot{\theta}_1(i)$	$\theta_2(i)$	$\dot{\theta}_2(i)$
0	0	-1	1	0
1	2	0	-3	0
2	-1	0	0	0

The following graphs present the obtained results. Figure 3 shows the temporal evolution of the position of joint 1 and Figure 4 his speed. Figure 5 shows the position of joint 2 and Figure 6 his respective speed.

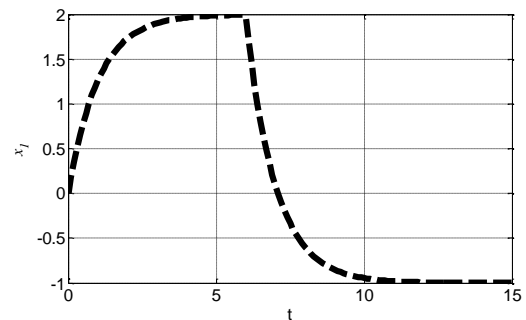


Figure 3. Position of joint 1

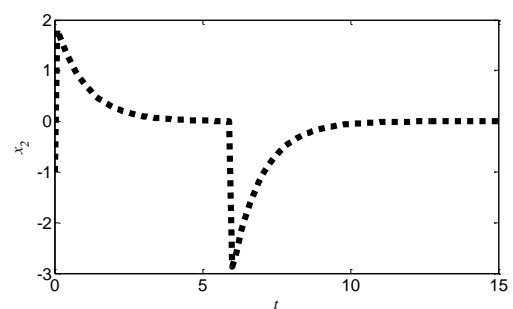


Figure 4. Speed of joint 1

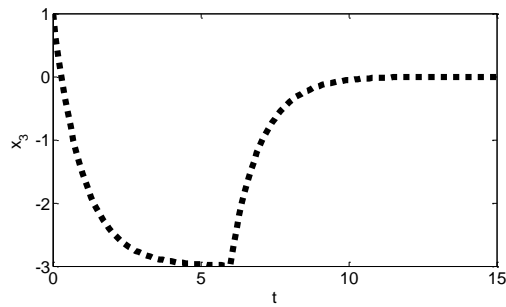


Figure 5. Position of joint 2

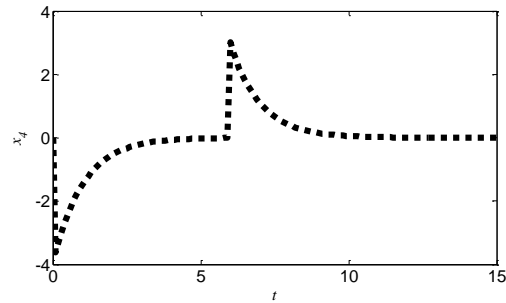


Figure 5. Speed of joint 2

### 3.2 Control of the direct current motor

In Table 3 can be seen the values for the motor of the first link, and in table 4 the values for the motor of the second link.

Table 3. Parameters of the motor from the first link.

$V_{\max}$	340 (V)
$I_{\max}$	16.5 (A)
$T_{\max}$	14.7 (Nm)
$R_a$	0.54 ( $\Omega$ )
$b$	$2.19(10^{-4})(\text{kgm}^2/\text{s})$
$K_e$	0.89 (Vs/rad)
$I$	0.012433647 ( $\text{kgm}^2$ )

In Figure 6 it can be observed the voltage variation to be applied to the motor of the link 1 to make him follow the trajectory proposed in Figure 3.

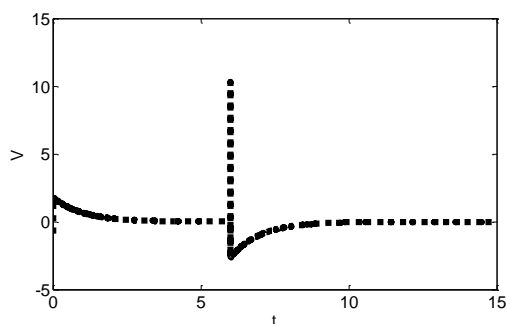


Figure 6. Voltage applied on motor 1

Table 3. Parameters of the motor from second link.

$V_{\max}$	48 (V)
$I_{\max}$	55 (A)
$T_{\max}$	2.6 (Nm)
$R_a$	0.14 ( $\Omega$ )
$b$	$2.19(10^{-4})(\text{kgm}^2/\text{s})$
$K_e$	0.113 (Vs/rad)
$I$	0.003606449 ( $\text{kgm}^2$ )

Figure 7 shows the voltage variation applied to the motor of the link 2 to move the same in the trajectory proposed in Figure 5.

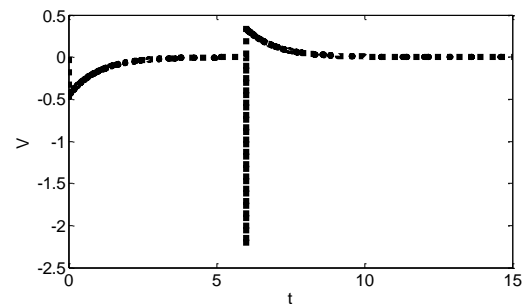


Figure 7. Voltage applied on motor 2

## 5 Conclusion

In this paper, a nonlinear control technique based on the State-Dependent Riccati equations applied to control the position and speed of a two link robotic manipulator is demonstrated. The graphs shown that the SDRE technique had success to control the position and speed of the two links of the manipulator, converging to the desired values even though the non-linearity's of the model

The values point to point obtained during the calculation are easily applied to obtain the curves of the voltage to be applied to the DC motor, which is responsible to insert the force in to the system.

## Acknowledgments

The author thanks CAPES, CNPQ, FAPESP and Fundação Araucária.

## Bibliography

- Cassiano, J. and Balthazar, J.M. (2007). On Homoclinic Chaos and a Control Chaos Strategy Applied to a Free-Joint Nonholonomic Manipulator. International Journal of Bifurcation and Chaos, Vol. 17, No. 6, pp. 2009-2020. DOI: [10.1142/S021812740701818X](https://doi.org/10.1142/S021812740701818X)
- Huifeng, C.; Hongxing, L. and Peipei, Y. (2009). Swinging-up and stabilization of the inverted pendulum by energy well and SDRE control, in:

- Proceedings of the Chinese Control and Decision Conference, pp. 2222-2226.
- Fenili, A. and Balthazar, J.M. (2010). The rigid-flexible nonlinear robotic manipulator: Modeling and control. *Commun Nonlinear Sci Numer Simulat*, Vol. 16, No. 5, pp. 2332-2341. DOI: [10.1016/j.cnsns.2010.04.057](https://doi.org/10.1016/j.cnsns.2010.04.057)
- Groover, M.P.; Weiss, M.; Nagel, R. and Odrey, N. (1987). *Industrial robotics: technology, programming, and applications*. McGraw-Hill.
- Hashemipour, S. H.; Karimi, H. and Adeli, A. (2013). Neural Network MLP with Sliding Mode Controller for Robotic Manipulator. *J. Basic. Appl. Sci. Res.*, Vol.3, No.1, pp. 512-520.
- Korayem, M.H.; Irani, M. and Nekoo, S.R. (2011). Load maximization of flexible joint mechanical manipulator using nonlinear optimal controller. *Acta Astronautica*, Vol. 99, No. 7-8, pp.458-469. DOI: [10.1016/j.actaastro.2011.05.023](https://doi.org/10.1016/j.actaastro.2011.05.023)
- Molter, A.; Silveira, O.A.A.; Fonseca, J. S. O. and Bottega, V. (2010). Simultaneous Piezoelectric Actuator and Sensor Placement Optimization and Control Design of Manipulators with Flexible Links Using SDRE Method. *Mathematical Problems in Engineering*, pp. 1-23. DOI: [10.1155/2010/362437](https://doi.org/10.1155/2010/362437)
- Tusset, A.M. ; Balthazar, J.M. ; Bassinello, D. ; Pontes Jr, B.R. and Felix, J. L. P. (2012). Statements on chaos control designs, including a fractional order dynamical system, applied to a MEMS comb-drive actuator. *Nonlinear Dynamics*, Vol. 69, No. 4, pp. 1837-1857. DOI: [10.1007/s11071-012-0390-6](https://doi.org/10.1007/s11071-012-0390-6)